Lawrence Berkeley National Laboratory
Recent Work

Title
SOME OBSERVATIONS ON THE AMORPHOUS TO CRYSTALLINE TRANSFORMATION IN SILICON

Permalink
https://escholarship.org/uc/item/8xp73218

Authors
Drosd, R.
Washburn, J.

Publication Date
1981-10-01

eScholarship.org Powered by the California Digital Library
University of California

LBL-13526 c.2
Preprint

Lawrence Berkeley Laboratory

UNIVERSITY OF CALIFORNIA

RECEIVED
LAWRENCE
BERKELEY LABORATORY

NOV 24 1981

LIBRARY AND
DOCUMENTS SECTION

Materials & Molecular Research Division

To be published in the Journal of Applied Physics

SOME OBSERVATIONS ON THE AMORPHOUS TO
CRYSTALLINE TRANSFORMATION IN SILICON

R. Drosd and J. Washburn

October 1981

TWO-WEEK LOAN COPY

This is a Library Circulating Copy
which may be borrowed for two weeks.
For a personal retention copy, call
Tech. Info. Division, Ext. 6782

Prepared for the U.S. Department of Energy under Contract W-7405-ENG-48

LBL-13526 c.2

DISCLAIMER

This document was prepared as an account of work sponsored by the United States Government. While this document is believed to contain correct information, neither the United States Government nor any agency thereof, nor the Regents of the University of California, nor any of their employees, makes any warranty, express or implied, or assumes any legal responsibility for the accuracy, completeness, or usefulness of any information, apparatus, product, or process disclosed, or represents that its use would not infringe privately owned rights. Reference herein to any specific commercial product, process, or service by its trade name, trademark, manufacturer, or otherwise, does not necessarily constitute or imply its endorsement, recommendation, or favoring by the United States Government or any agency thereof, or the Regents of the University of California. The views and opinions of authors expressed herein do not necessarily state or reflect those of the United States Government or any agency thereof or the Regents of the University of California.

SOME OBSERVATIONS ON THE AMORPHOUS TO CRYSTALLINE TRANSFORMATION IN SILICON

R. Drosd and J. Washburn

Materials and Molecular Research Division
Lawrence Berkeley Laboratory
University of California
Berkeley, California 94720

ABSTRACT

An atomistic model for the transformation of amorphous (α) to crystalline silicon films while in contact with a crystalline substrate is presented. The atomic structure of the {100}, {110}, and {111} surfaces is examined and related to the observed interface migration rates. The assumption that for an atom to attach successfully to the crystal it must complete at least two undistorted bonds leads to the prediction that the {100} amorphous/crystalline interface should advance fastest and the {111} slowest. The origin of crystal defects is discussed in terms of the atomistic recrystallization mechanism. Microtwins are found to be a logical consequence of crystallization on the {111} surfaces but are not expected to form on any other interface. Once microtwins are formed they can increase the recrystallization rate of a {111} surface. This phenomenon is both described in the model and experimentally observed.

This work was supported by the Office of Basic Energy Sciences through The Materials and Molecular Research Division of the U.S. Department of Energy under Contract No. W-7405-ENG-48.

INTRODUCTION

The regrowth of thin amorphous (α) silicon films, formed during ion implantation on the surface of Si wafers, has been studied by many investigators (1,2,3,4,5,22). During annealing crystal growth takes place by the motion of the amorphous/crystalline (α/C) interface. The interface migration rates and the lattice defects produced during annealing have been found to depend on the crystal substrate orientation, the implantation temperature, and the implanted element. If the α layer is formed during low temperature phosphorus ion implantation microtwins are observed (6) in annealed {111} wafers whereas in a {100} wafer only dislocation loops (7) are found (see Fig. 1). When the α layer is created during a 100°C or higher implantation, annealing yields a dense tangle of dislocations for both orientations. Heating due to the ion beam may be sufficient to cause this temperature rise. Once above the amorphitization level, the implantation dose in this case affects the density but not the type of defects produced during annealing. The {110} substrate has also been studied but is very similar in its defect structure to {100}. The results given above also apply to silicon implantation into silicon.

The regrowth rates for α layers have been reported for the <100>, <110>, and <111> directions by several workers (8,9). Crystallization in the <100> direction is fastest followed by <110> and then <111> which are about 2.3 and 20 times slower, respectively, as shown in Fig. 2. To our knowledge amorphous-crystalline interface migration rate measurements have been made only on low temperature implanted

specimens. The data presented in Fig. 2 was obtained from a new experimental technique described elsewhere (10). Amorphitization was accomplished by implanting phosphorus at 100 keV to 10^{16} ions/cm^2 at 77°K. The apparent activation energy for interface migration was 2.9 ± 1 eV. Other workers (11,12) have reported values of 2.4 eV and 2.9 eV.

The experimental observations mentioned above have, for the most part, been known for some time. However, until very recently there had been little success (11) in the development of a model that could explain the way in which the recrystallization rate and defect microstructure were affected by the substrate orientation and the implantation temperature.

Csepregi et al. (13) have recently proposed a mechanism that attempts to explain the differences in α layer regrowth rates on {111} and {100} substrates. However, Csepregi's model cannot account for regrowth rate in the <110> direction. In addition there was only a brief consideration of the formation of lattice defects during interface migration.

Spaepen et al (21) gave proposed an atomistic model of the bond arrangements in the amorphous phase at the {111} α/C interface. In addition, they show how bonds can be broken so that atoms may be transferred from the α to the crystalline phase of defects on a perfect {111} surface.

We present a model that is in some respects similar to that of Spaepen. However, the atomic bond structure in the α phase is not

considered in detail for reasons of clarity. This has allowed us to examine additional orientations of the α/C interface as well as the effect of twinning on interface migration. The atomic mechanism of α/C interface migration is based on the criterion that atoms of the α phase must make two undistorted bonds with the crystal before they are considered to belong to the latter phase. Undistorted bonds are those with the characteristic length and angle of the crystalline phase. Using this approach it will be shown that qualitative prediction of crystallization rates of several orientations can be made. In addition some rather detailed predictions of defect microstructure resulting from α layer recrystallization will be presented.

It is interesting to note that Spaepen (21) considered the criterion for atomic incorporation in the crystalline phase as the completion of a sixfold ring of atomic bonds, characteristic of the diamond cubic structure. It will be shown that this and the present approach lead to the same conclusions.

Discussion of Results

Layers of α silicon, in contact with a crystalline substrate, crystallize by the motion of the interface rather than by nucleation of new crystals within the α phase (10). This result is in agreement with the work of Blum (14) and Turnbull (22) where it was found that the time required for nucleation of new crystals in α silicon is extremely long in the temperature range of interest here. For the α/C interface to advance during annealing single atoms or small groups of atoms reorient at the amorphous-crystal interface so as to add to the

crystal surface at a correct location and orientation. For an atom to be considered part of the crystal it must have formed at least two undistorted bonds to the crystal (15). The exact crystal growth mechanism will depend on the orientation of crystallographic face involved.

Figure 3 shows a block of diamond cubic material. The front surface is a $<\bar{1}10>$ projection while the three upper surfaces, (110), (111), and (101) are shown three dimensionally. In this drawing the process of nucleation of new atomic layers on the crystal is shown for the three primary crystal surfaces. The requirement that an atom complete two undistorted bonds to the crystal to successfully bond to it poses no problem on the (001) surface. Here it is seen that a single atom forms two bonds to the crystal atom arriving at the surface. While the remaining two bonds will be made to atoms in the α phase or possibly remain unsatisfied. On a flat (110) surface a cluster of two atoms is necessary such that each atom completes two undistroted bonds (one to an atom in the crystal and one to the other atom in the cluster). On the (111) surface nucleation of a new layer is even more difficult since clusters of three atoms are required. These surface cluster are nuclei for new atomic layers and are thus labeled "N" in Figure 3. Further growth can taken place more easily by expanding on the established nucleus rather than by producing more nuclei on the {110} and {111} surfaces.

Expansion of the surface nuclei on (110) and (111) is shown in Figure 3. On (110) single atoms may attach to the two atom nucleus and complete two undistorted bonds. In doing so they form a linear

chain along the surface in a <110> direction. On the (111) surface the three atom nucleus may expand first by the addition of a single atom but then must be followed by a two atom cluster such that the two bond per atom requirement is met. This chain of atoms may branch off in several directions on the surface. On {100} surfaces single atoms may be incorporated and therefore no nucleation step is required.

The requirement of two completed bonds for atomic additions to the crystal is seen three dimensionally on the (110), (111), and (001) surfaces. On the opposite surfaces, $(00\bar{1})$, $(\bar{1}\bar{1}0)$, and $(\bar{1}\bar{1}\bar{1})$, the [110] projected image of these additions is indicated by cross-hatching. Here the two bonds per atom requirement is more easily seen to be satisfied.

It is interesting to note that Shaepen et al (21) considered the basic criterion for crystal growth to be the formation of six-fold rings, characteristic of the diamond cubic structure, at the α/C interface. This is an alternative approach to the two bond per atom requirement first proposed by Faust and John (15). It can be seen, however, from the $(\bar{1}\bar{1}\bar{1})$, $(\bar{1}\bar{1}0)$, and $(00\bar{1})$ faces in figure that the three, two, and one atom clusters are completing six-fold rings (cross-hatched areas) at the α/C interfaces. When nucleation of a new atomic layer is accomplished on a flat α/C, interface the incoming atom(s) will complete a ring that is inclined to the interface. In doing so the atom(s) will also complete two undistorted bonds to the crystal.

An alternative way of looking at the relative difficulty of atomic growth on different crystal faces is to consider how much of a yet to be completed six-fold ring is "submerged" within the crystal. On the {100} surface it is seen in Figure 3 that only one corner of the ring extends above the surface and hence only one atom is required to complete it. On the {110} surface one side of the ring protrudes out of the surface and two atoms are needed to complete it. On the {111} surface one half of the six-fold ring is exposed and hence three atoms are needed to finish it off.

Reconstruction and Atomic Roughness of the Crystal Surface

Surface reconstruction is known to occur when silicon is in contact with its melt or vapor (16). Amorphous silicon, unlike the liquid or vapour phases is still covalently bonded. Therefore rigidly fixed bonding is probable across an α/C interface making reconstruction most unlikely. The diamond cubic structure is probably maintained right up to the α/C interface. The figures presented in this paper are based on this assumption.

Whether or not the interfaces are atomically flat is also important to the growth process. An atomically rough {111} surface will contain many steps at which growth can occur by attachment of single atoms without the need for repeated nucleation (17) of growth steps. Jackson has predicted from thermodynamic arguments that the {111} face will be smooth and the {100} rough when in contact with the melt at (1410°C). However, these conclusions are of little help in predicting the structure of the amorphous to crystalline interface. However, we will assume that an atomically flat interface will have the lowest free energy.

Prior to the start of annealing of an α layer the degree of roughness at the α/C interface is determined by the amorphitization process. Once annealing begins and significant atomic motion becomes possible the "equilibrium" degree of roughness should be attained quickly.

The Origin of Defects in Recrystallized Layers

Primarily two types of secondary defects are observed as a result of recrystallization of α silicon layers, dislocations and microtwins. Dislocations are a result of point defects that condense to form dislocation loops or the impingement of α-C interfaces where the two crystal fronts are out of registry. The loops may grow large enough that they intersect each other thus forming a tangle or network. Point defects are formed during the implantation process as each incident ion creates vacancies and interstitials. Just prior to annealing many of these primary defects reside in the crystalline silicon near the α/C interface. Dislocation loops found after annealing are at a depth in the specimen approximately equal to the original α layer thickness. Hence, the primary defects formed during implantation are responsible for the majority of the dislocation loops.

Microtwins are nucleated at the α/c interface. The clusters of three atoms required on {111} faces may bond in two different positions as shown in Fig. 3. The cluster labeled "correct" has attached in a position that continues the correct stacking order of {111} planes. The nucleus labeled "twin" has reversed the stacking order and is thus the beginning of a twin. No first nearest neighbor mistakes have been made by the twin cluster and hence the excess energy of this defect is

small. Similar stacking mistakes on the (100) and (110) surfaces require first nearest neighbor mistakes and are thus unlikely to occur. Experimentally microtwins are only observed for <111> regrowth (7). It is easily visualized how twins in the plane of the α/C interface might arise. However, microtwins on inclined {111} planes are observed as well (6). These twins may be accounted for by assuming that the original interface is not planar over large areas. "Bumps" or long range irregularities probably exist as shown in Fig. 4 (although the α/C interface is smooth on an atomic level). Upon annealing the sides of these hills should become bounded by inclined {111} planes since [111] is the slowest regrowth direction. This would lead to the possibility of stacking mistakes on inclined {111} planes by the same mechanism as mentioned above.

The Effect of Microtwins on the Migration of a {111} Interface

Microtwins, once formed on inclined {111} planes, can accelerate the crystal growth process. The rate controlling step for growth in the <111> direction is probably nucleation of new atomic ledges, requiring simultaneous positioning of three atoms on the crystal lattice sites on a defect free surface. As has been pointed out by many investigators (15,18,19,20), the point of exit of a twin boundary at the crystal surface can act as a nucleation site for atomic steps. At this boundary on a {111} surface only two atoms are required to establish a nucleus as shown in Fig. 5. Once a segment of the twin boundary, at its intersection with the α/C interface, has been decorated with two-atom clusters, a linear growth step has been

created. This step can propagate by the addition of single atoms in a direction perpendicular to itself, <211>. Only one of the two twin boundaries will be effective in accelerating the growth on the adjacent {111} surface. This is because an atomic ledge on a {111} surface aligned along <110> has a fast and slow <211> growth direction as shown in Fig. 6. In the fast direction single atoms may attach at the step but in the slow direction a two atom nucleus, followed by single atom attachment, is required to advance the atomic step by one row. The right hand twin boundary in Fig. 5 nucleates an atomic step that can expand in the fast direction for the matrix as well as on the twin. At the left twin boundary in Fig. 6 the growth step has to expand in the slow direction both in the matrix and on the twin. Therefore, the {111} crystalline surface should attain an enhanced growth rate primarily on one side of the twin. The resulting exposed lateral surface of the twin (marked S in Fig. 7) can migrate slowly resulting in an increase in thickness of the twin but must do so by nucleating new atomic layers. The other side surface of the twin is never exposed at the fast growing boundary. Experimentally, the microtwins are observed to thicken primarily from one side as shown in Fig. 8. The twins have one planar boundary while steps are seen on the opposite side where the twin increases in thickness. The planar twin boundary has advanced further than the other, as the model predicts.

Csepregi et al. (13) have presented a mechanism by which microtwins may increase the {111} interface migration rate during annealing. They proposed that since the exposed surface of the twin is initially {511}

it will be able to grow much faster than the surrounding {111} matrix surface. The {511} surface is close to {100} and hence should achieve a high growth rate initially. However, the protruding twin should soon become bounded by its slow growing {111} faces as shown in Fig. 9. Once this has occurred the twin will not be able to grow faster than the matrix, except by the mechaism mentioned above.

The Activation Energy for Recrystallization

The activation energy for α/C interface migration is in dispute at the present time (10,11,12). However, the fact that the activation energy is constant for a variety of recrystallization directions has been confirmed (11). This observation may seem unusual since growth on the {111} surface requires nucleation of atomic steps while on the {100} surface single atoms should be able to attach independently. This suggests that the thermally activated event for growth on any surface is similar - perhaps the reorientation of a small group of atoms in the amorphous material at the interface as proposed by Spaepen (21). The different growth rates reflect the different probabilities that such an event will result in placement of atoms in position to form new regular bonds to the crystal. It is puzzeling that all reported measurements of α layer crystallization activation energy are well in excess of that for self diffusion.

The Effect of the Implantation Temperature and the Implanted Ion Species on α/C Interface Migration

α layers created during implantation at elevated temperatures of about 100°C recrystallize differently than those resulting from 77°K ion bombardment. Most notably a high temperature implanted {111}

substrate containing an α layer will not produce twins when annealed. To determine the effect of the implantation temperature on the α layer dark filed micrographs were taken of samples that were implanted but unannealed, as seen in Fig. 10. This figure suggests that the α/C interface is rougher when the implantation is carried out at higher temperatures. There may even be small islands of the original crystal remaining throughout the α layer. If this is the case the growth direction becomes less well defined; many segments of the α/C interface will initially be migrating in directions other than that normal to the wafer plane during annealing. In this fashion a nominally {111} interface would at first be able to avoid propagation in the <111> direction. The thin α layer (~1000 Å) created by ion implantation may be completely recrystallized before it can become planar and start to produce twins. Another possible difference (between high and low temperature implanted silicon) is the initial level of internal stress at the interface. Stresses at the interface may play a role in microtwin nucleation.

It has been reported (11) that the type of ion used to form the α layer can substantially affect the migration rate, activation energy, and final defect microstructure. If reorientation of a small group of atoms in the amorphous material is the rate controlling step then segregation of impurities at the interface or their random distribution in the amorphous material could facilitate the necessary bond breaking or influence the nucleation and propagation of growth steps.

Conclusions

1. At {111} α/C interfaces microtwins on inclined {111} planes accelerate the crystal growth process by providing sites of easy nucleation of growth ledges at one of the twin boundaries.

2. The activation energy measured for α/C interface migration probably relates to reorientation of small groups of atoms in the a/C interface.

3. Relative α/C interface migration rates in the three major cubic directions can be understood in terms of the probability that a suitable site for attachment will exist when an atom group shifts from one orientation to another in the α/C interface.

4. The implantation temperature affects the α/C interface morphology and perhaps the structure of the α layer itself.

5. Microtwins are not formed when thin amorphous layers produced by hot implantation of {111} specimens are epitaxially regrown.

Acknowledgement

This work, including that reported in a previous paper (Ref. 10), was supported by the Department of Energy, Office of Basic Energy Sciences through the Materials and Molecular Research Division of the Lawrence Berkeley Laboratory under Contract No. W-7405-ENG-48. The authors regret the inadvertent omission of an acknowledgement in Ref. 10.

REFERENCES

1. H. Kraütle, Rad. Eff. 24, 255, (1975).

2. H. Muller, W. Chu, J. Gyulai, J. Mayer, T. Sigmon, T. Cass, App. Phys. Lett. 26, 292, (1975).

3. C. Cristodoulides, R. Baragiola, D. Chivers, W. Grant, J. Williams, Rad. Eff. 36, 73, (1978).

4. E. Kennedy, L. Csepregi, J. Mayer, J. App. Phys. 48, 4241, (1977).

5. L. Csepregi, E. Kennedy, T. Gallagher, J. Mayer, J. App. Phys. 48, 4234, (1977).

6. M. Rechtin, P. Pronko, G. Foti, L. Csepregi, E. Kennedy, J. Mayer, Phil. Mag. (A) 37, 605, (1978).

7. R. Drosd, Ninth International Congress on Electron Microscopy, edited by J. Sturgess (1978), p. 384, published by Microscopical Society of Canada, Toronto.

8. J. Brice, P. Wiffin, Sol State Elec. 7, 183, (1964).

9. L. Csepregi, J. Mayer, T. Sigmon, App. Phys. Let. 29, 92, (1976).

10. R. Drosd, J. Washburn, J. App. Phys. 51, 4106, (1980).

11. S. Lau, J. Vac. Sci. Tech. 15, 1656, (1978).

12. U. Kooster, Phys. Stat. Sol (b) 48, 313, (1978).

13. L. Csepregi, E. Kennedy, J. Mayer, T. Sigmon, J. App. Phys. 49, 3906 (1978).

14. N. Blum, C. Fledman, J. Non Cryst. Sol. 11, 242, (1972).

15. J. Faust, H. John, J. Phys Chem Sol. 23, 1119, (1962).

16. J. Van Vechten, J. Vac. Sci. Tech. 14, 992, (1977).

17. K. Jackson, Kinetics of Reaction in Ionic Systems, Plenum Press (1969), p. 229.

18. R. Seidensticker, D. Hamilton, J. App. Phys. 34, 3113, (1963).

19. A. Bennett, R. Longini, Phys. Rev. 116, 53, (1959).

20. D. Hamilton, R. Seidensticker, J. App. Phys. 31, 1165, (1960).

21. F. Spaepen, D. Turnbull, "Laser-Solid Interactions and Laser Processing: edited by S. Ferris et al., AIP Conf. Proceedings 50, 73 (1979).

22. D. Turnbull, Contemp. Phys. 10, 473, (1969).

FIGURE CAPTIONS

Figure 1. TEM micrographs of amorphous layers recrystallized at 800°C for 1/2 hour. Amorphitization was a result of an 100 keV phosphorus ion implantation to a dose of $10^{16}/cm^2$. Figures a. and b. are {100} and {111} substrates, respectively, implanted at 100°C. Both exhibit a dislocation network as well as a few dislocation loops. Figures c. and d. are also {100} and {111} orientations but were implanted at 77°K. The {100} sample has a low density of dislocation loops while the {111} samples has a high density of microtwins. The inset {110} diffraction pattern, showing strong twinning relfections, was obtained by tilting the {111} sample.

Figure 2. A plot of amorphous layer regrowth rate versus reciprocal temperature. The activation energy is 2.9 eV for all three growth directions. <100> is fastest followed by <110> and then <111> which are 2.3 and 20 times slower, respectively. Phosphorus ions were used to form the amorphous layer.

Figure 3. A schematic drawing of the growth process on the major surfaces of a diamond cubic crystal is shown. The front face of the crystal is a $[1\bar{1}0]$ projection. Here the apparently "shorter" (horizontal) atomic bonds are actually inclined to the front surface. The minimum stable surface nucleus for each orientation is shown in cross hatching at the bottom. A twin cluster is also shown on the $(\bar{1}1\bar{1})$ surface. On the top and right surfaces of the crystal

surface nuclei, labeled "N" on the (111) and (110) surfaces, are seen to contain three and two atoms, respectively. The atoms, or atom clusters, circled and numbered indicate the order in which they would add on to the established nucleus. A twin nucleus, labeled "T", is shown on the (111) surface. Since atoms add on individually on the (001) surface, no nucleation step or sequential growth, occurs.

Figure 4. Schematic drawing of the {111} α/C interface. In fig. a. the unannealed interface is rough due to the amorphitization process. In fig. b. the interface, after being slightly annealed, has migrated a small distance and is now bounded by its slowest growing faces, {111}. Further growth will require nucleation of new atomic ledges which can result in stacking mistakes. In fig. c. the completely recrystallized α layer contains twins on all {111} planes as a result of the stacking mistakes made during growth.

Figure 5. A schematic drawing of a diamond cubic crystal containing a microtwin. The front surface is a [110] projection while the top shows the (111) matrix surface. At the right hand twin boundary the minimum size surface nucleus is seen to be two atoms (labeled "N") instead of the usual three for a defect free {111} surface. The atomic ledge, created at the twin boundary, expands by single atom additions as numbered in order.

Figure 6. A schematic drawing of an atomic ledge on the $(11\bar{1})$ surface of a defect free crystal. The ledge may expand in the [112] direction by the addition of single atoms. In the $[\bar{1}\bar{1}2]$ direction a nucleation step is required for the ledge to advance where a two atom cluster labeled "N" is shown. Single atoms may add to complete this row and then another nucleus must be formed for further growth. The numbered atoms indicate the order in which they attach to the crystal.

Figure 7. A schematic drawing of growth of an inclined microtwin at a {111} α/C interface. In fig. a. the twin boundary marked "A" is nucleating atomic ledges while "B" is not. This leaves the left side of the microtwin, marked "S", exposed to the amorphous material. In fig. b. the α/C interface has advanced only on the right side of the twin. In addition a new atomic ledge has nucleated on the exposed surface "S" of the microtwin, thus increasing its thickness. Figure c. shows atomic ledges being "sent over" from an unseen twin to the left of the drawing. In fig. d. it is seen that the twin has increased in thickness on one side only and on the other planar side the α/C interface is somewhat ahead.

Figure 8. A bright field TEM micrograph of recrystallization of α silicon in the [111] direction, the specimen plane is $(1\bar{1}0)$. Microtwins inclined to the α/C interface are seen on the $(11\bar{1})$ plane. The right hand twin boundaries are planar

while the left boundaries have steps. In addition the α/C interface is further advanced on the right side of the twins then on the left. This compares well to Fig. 7. The diffraction pattern shows twin reflections in addition to streaking indicating the twins are plate like. The small linear objects alligned along the (111) plane are twins parallel to the plane of the α/C interface. These twins are always small compared to the inclined twins since growth at their edges is in a perpendicular direction to that of the advancing crystal matrix. Within the larger inclined twins smaller linear objects are also seen. Those that are parallel to the $(11\bar{1})$ matrix planes are microtwins that have twinned back into the original orientation. Secondary twins are seen within the three large primary twins. These are regions that are twin oriented to the primary twin but have not returned to the matrix orientation.

Figure 9. Schematic drawing of the initial stages of growth of the surface of a microtwin. The matrix α/C interface is (111) but that of the twin is (511). The twin surface advances more rapidly than that of the matrix but then becomes bounded by the slow growing {111} planes. Once the configuration in fig. c. is obtained the microtwin can still aid crystallization but only by the twin boundary mechanism illustrated in Fig. 5, 7, and 8.

Figure 10. Figures a. and b. are dark field TEM micrographs of wedge shaped samples containing α layers that have not been annealed. The implantation temperature was 100°C for sample a. and 77°C for sample b. The bottom portion of each micrograph is the area near the central hole in a TEM specimen and thus represents the top surface of the implanted wafer. The lower inset diffraction patterns verify that this area is completely amorphous. In the upper portion of figs. a. and b. the crystalline substrate overlaps the α layer. The diffraction patterns show both crystalline reflections and amorphous like diffuse rings. Bright spots are seen in images a. and b. where the α layer and crystal substrate overlap, while none are seen where the α layer stands alone. We believe that these bright spots are strained crystalline zones in the α/C interface, as shown schematically in fig. c. The fact that the spots are much larger and show greater contrast in the sample implanted at the higher temperature indicates that the α/C interface roughness is on a much larger scale.

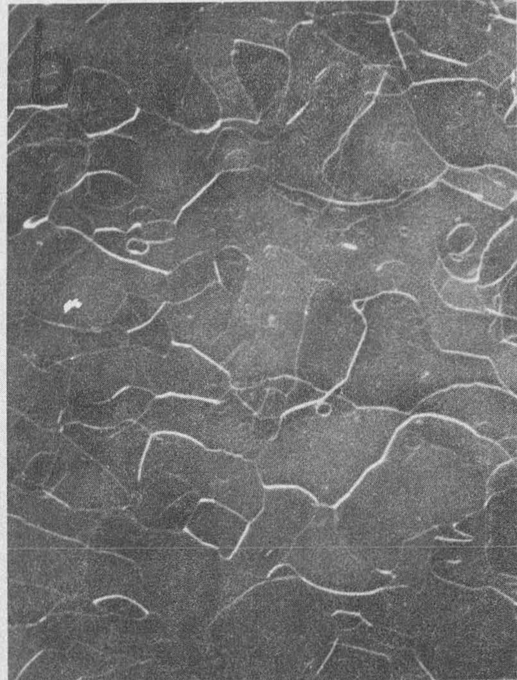

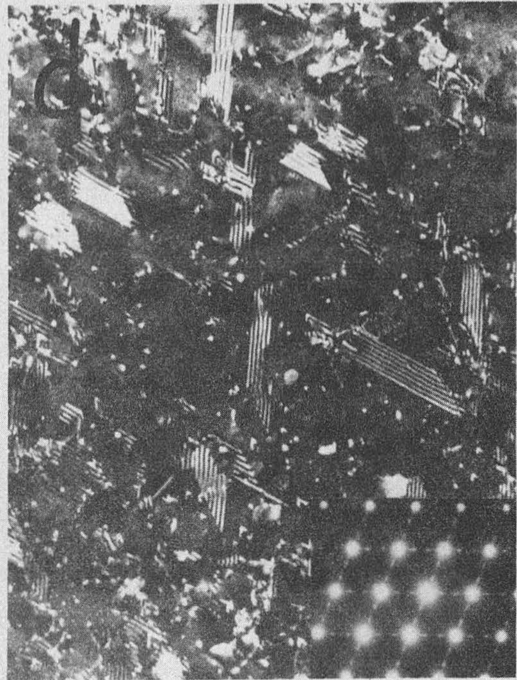

Fig. 1

XBB 802-1831

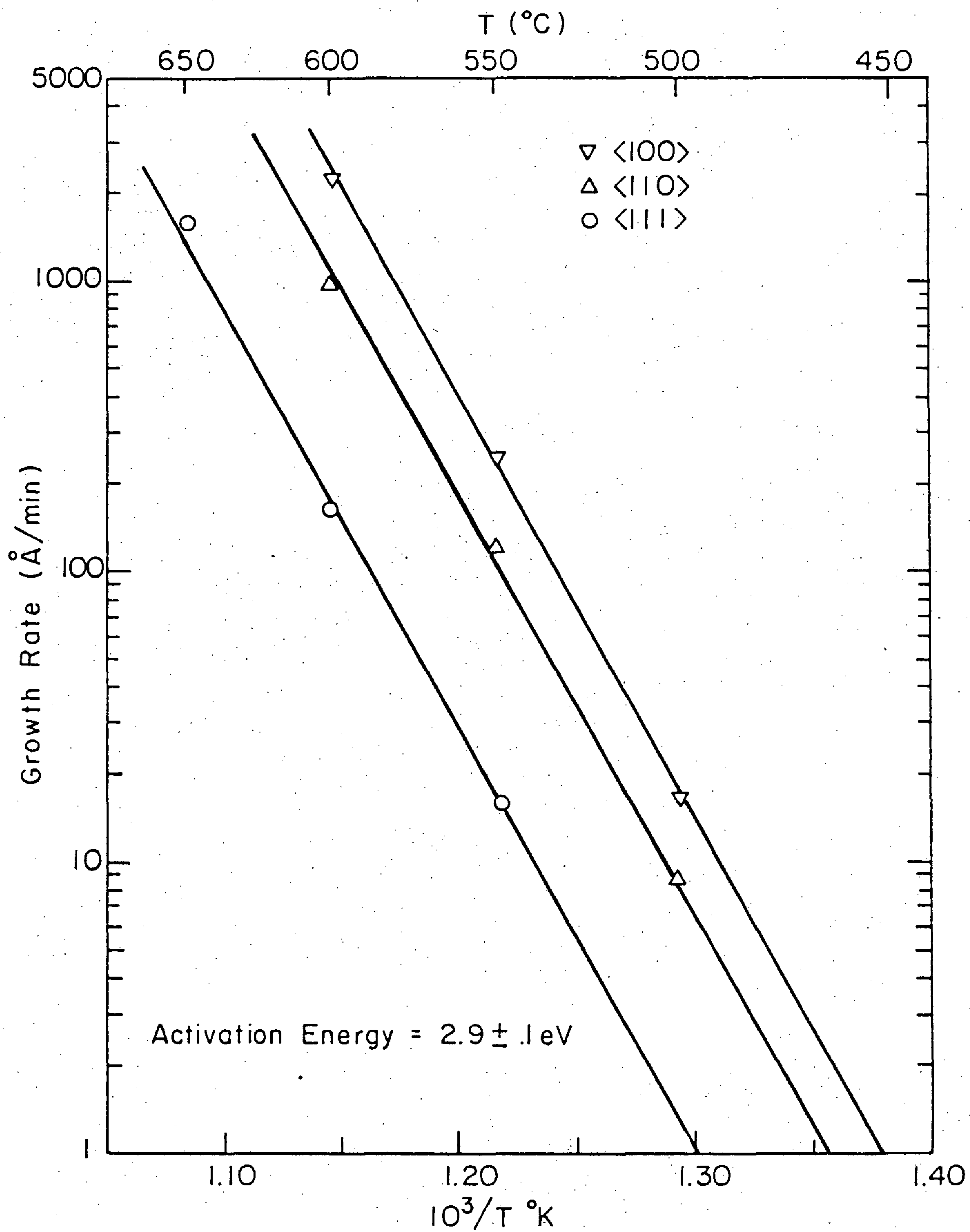

Fig. 2

XBL 799-7165

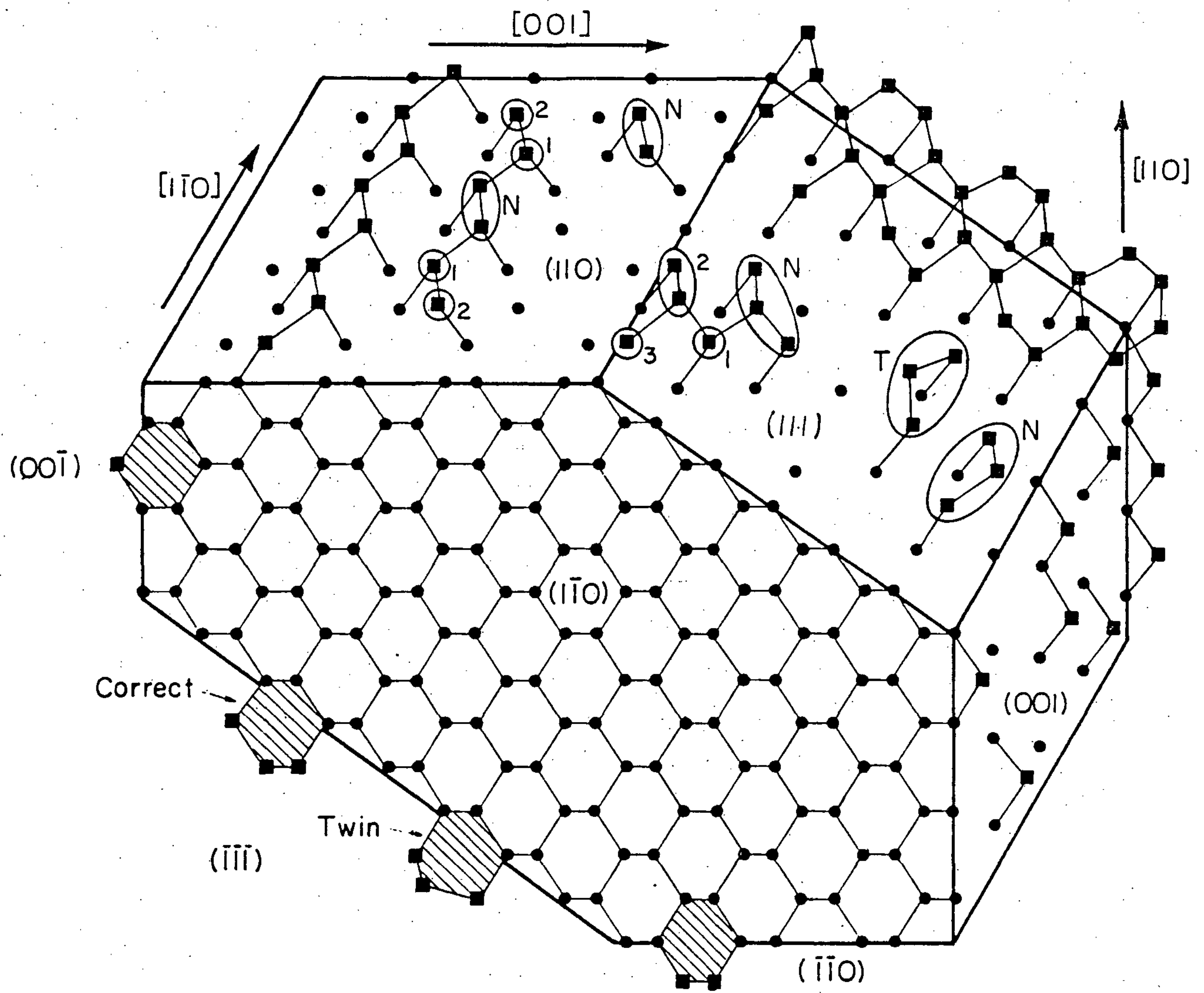

Fig. 3

XBL 803-4851

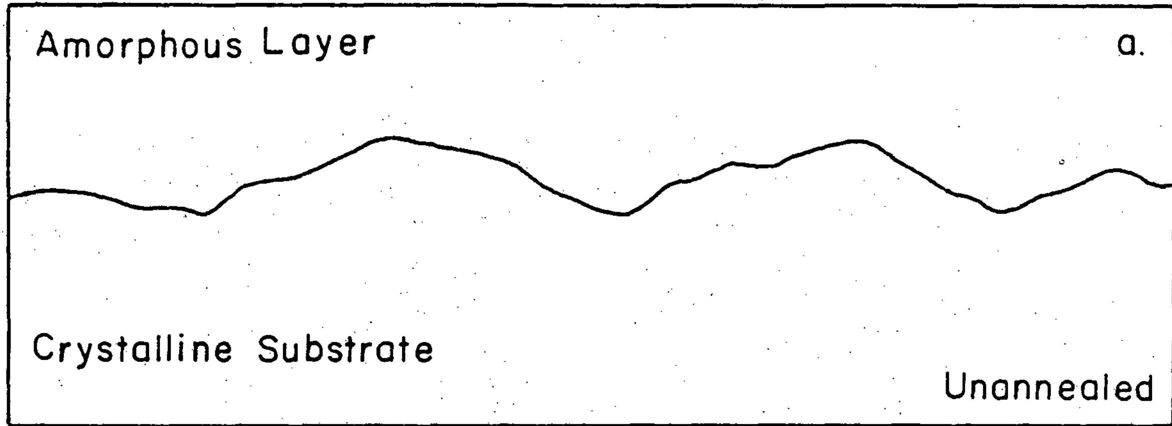

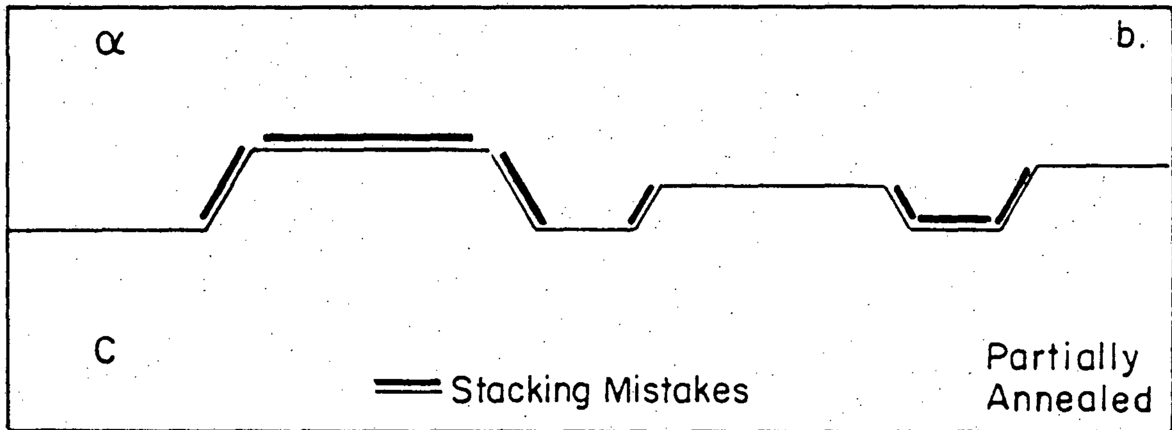

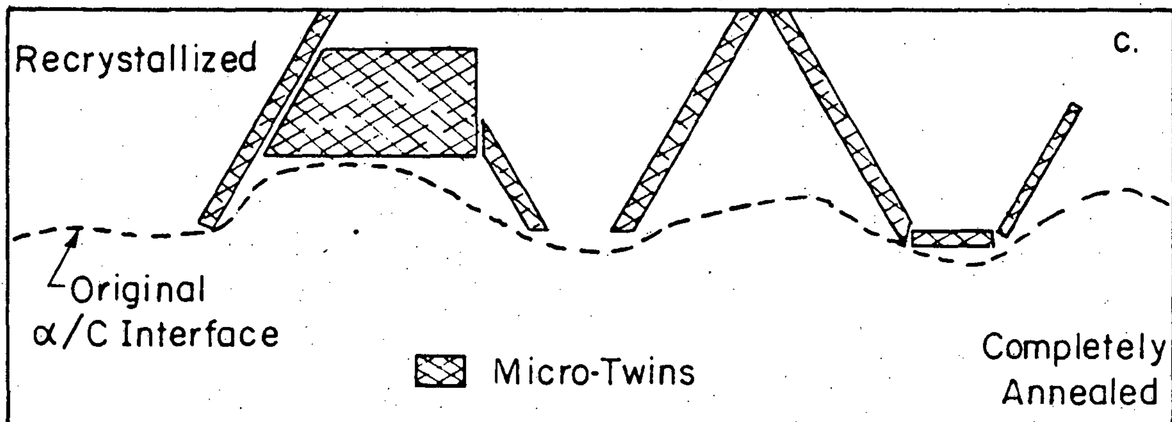

Fig. 4

XBL 799-7161

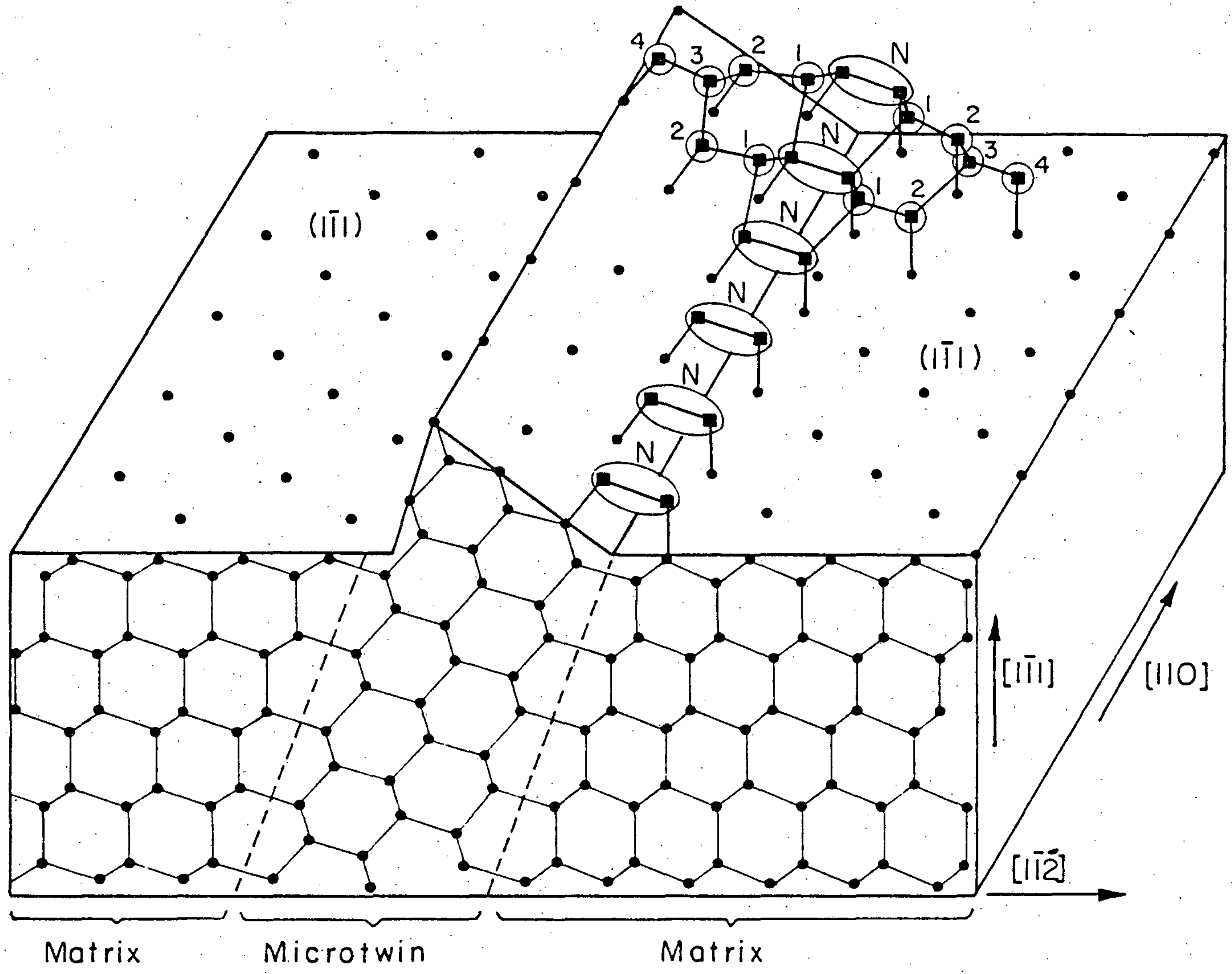

Fig. 5

XBL803-4852

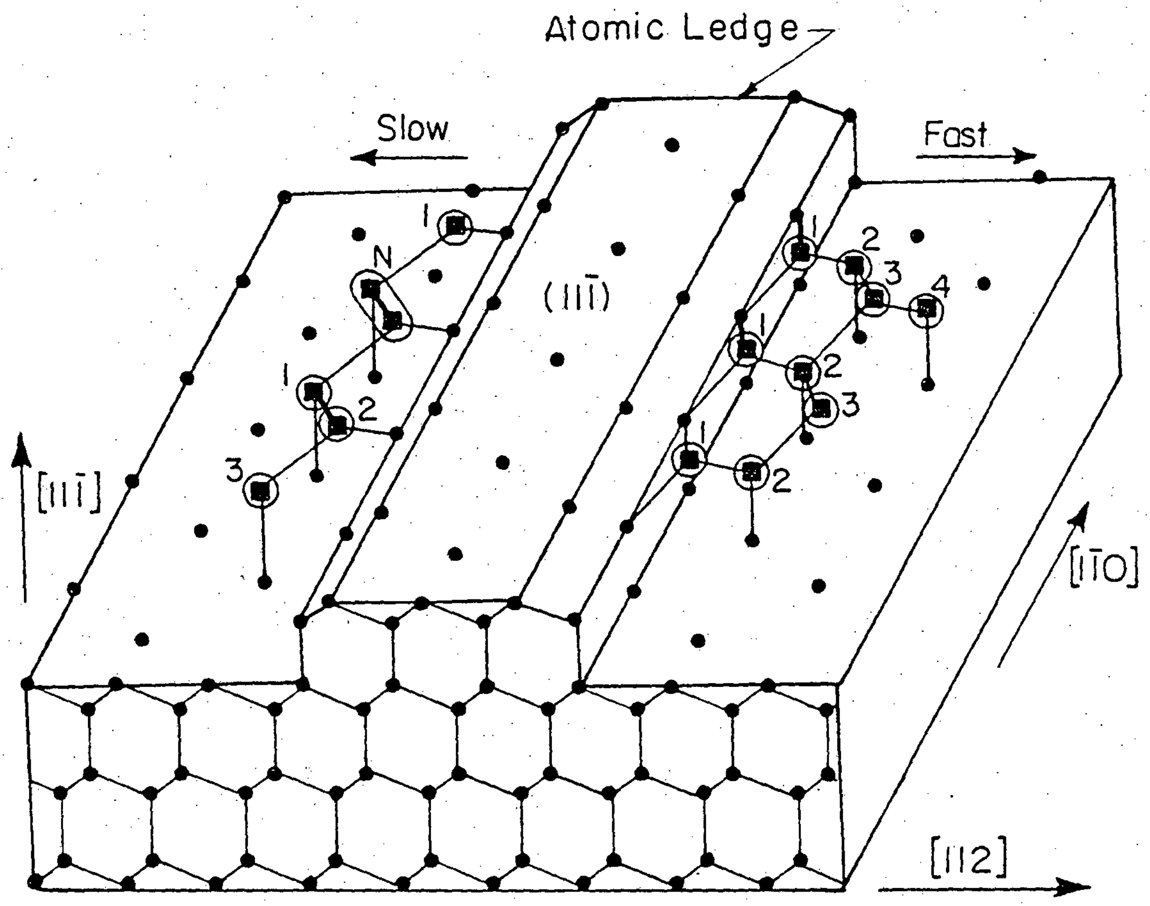

Fig. 6

XBL803-4850

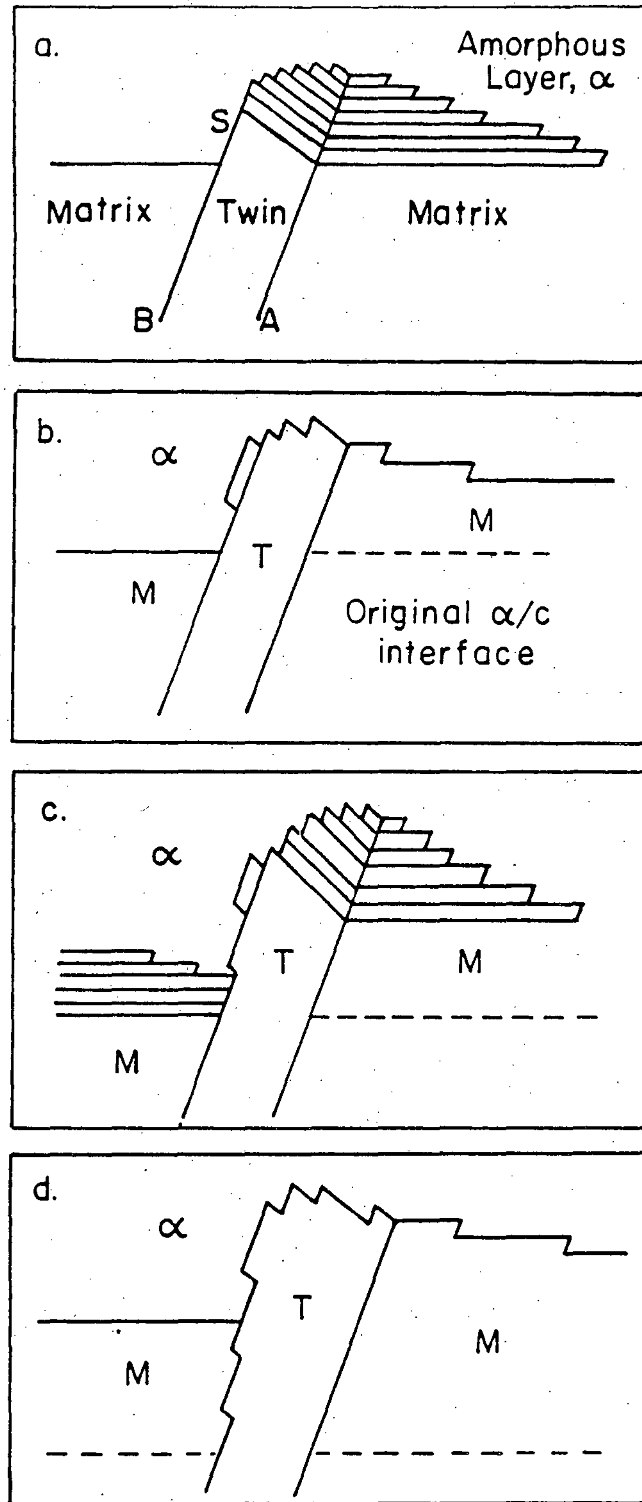

Fig. 7

XBL 803-4849

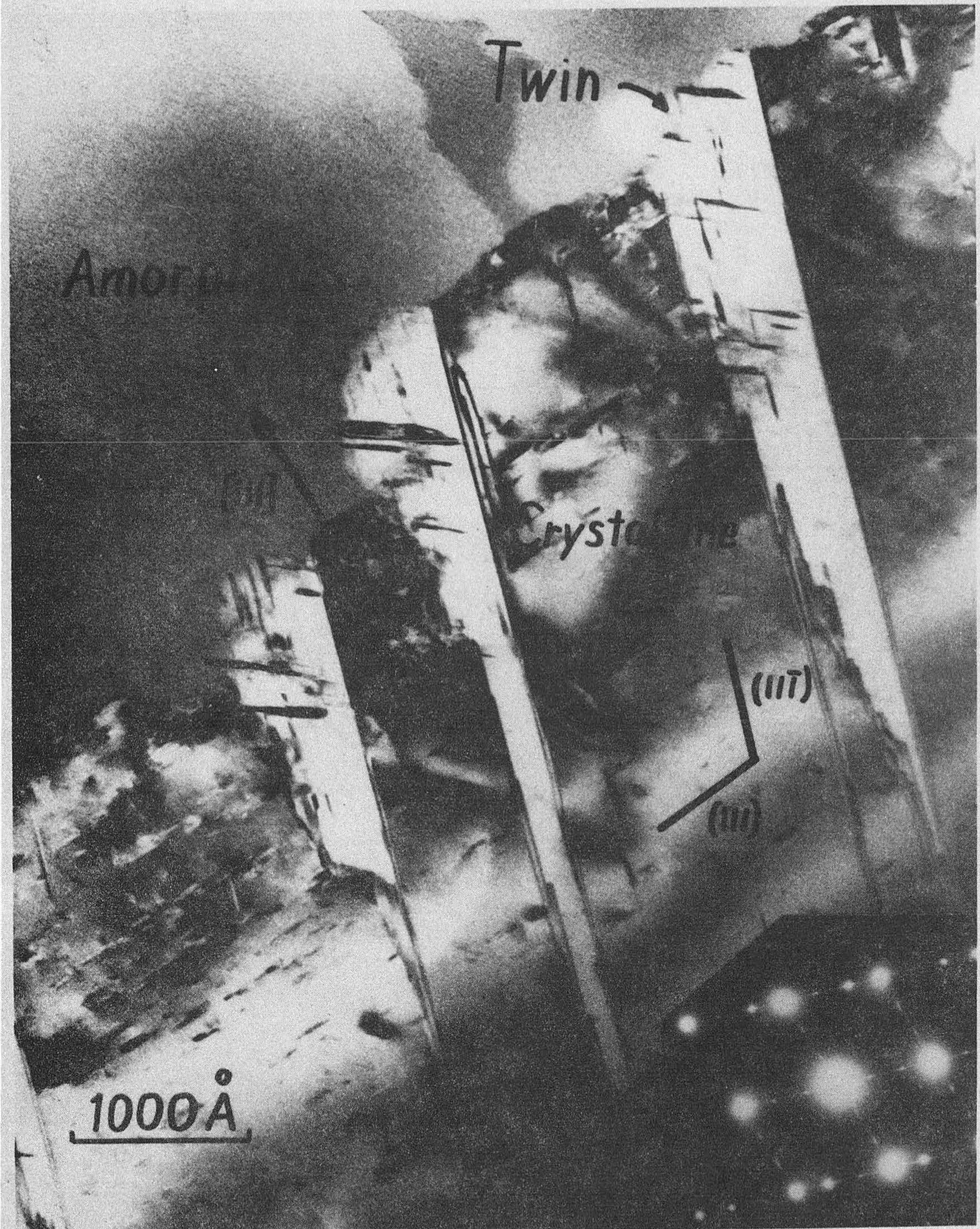

Fig. 8 XBB 7911-15623

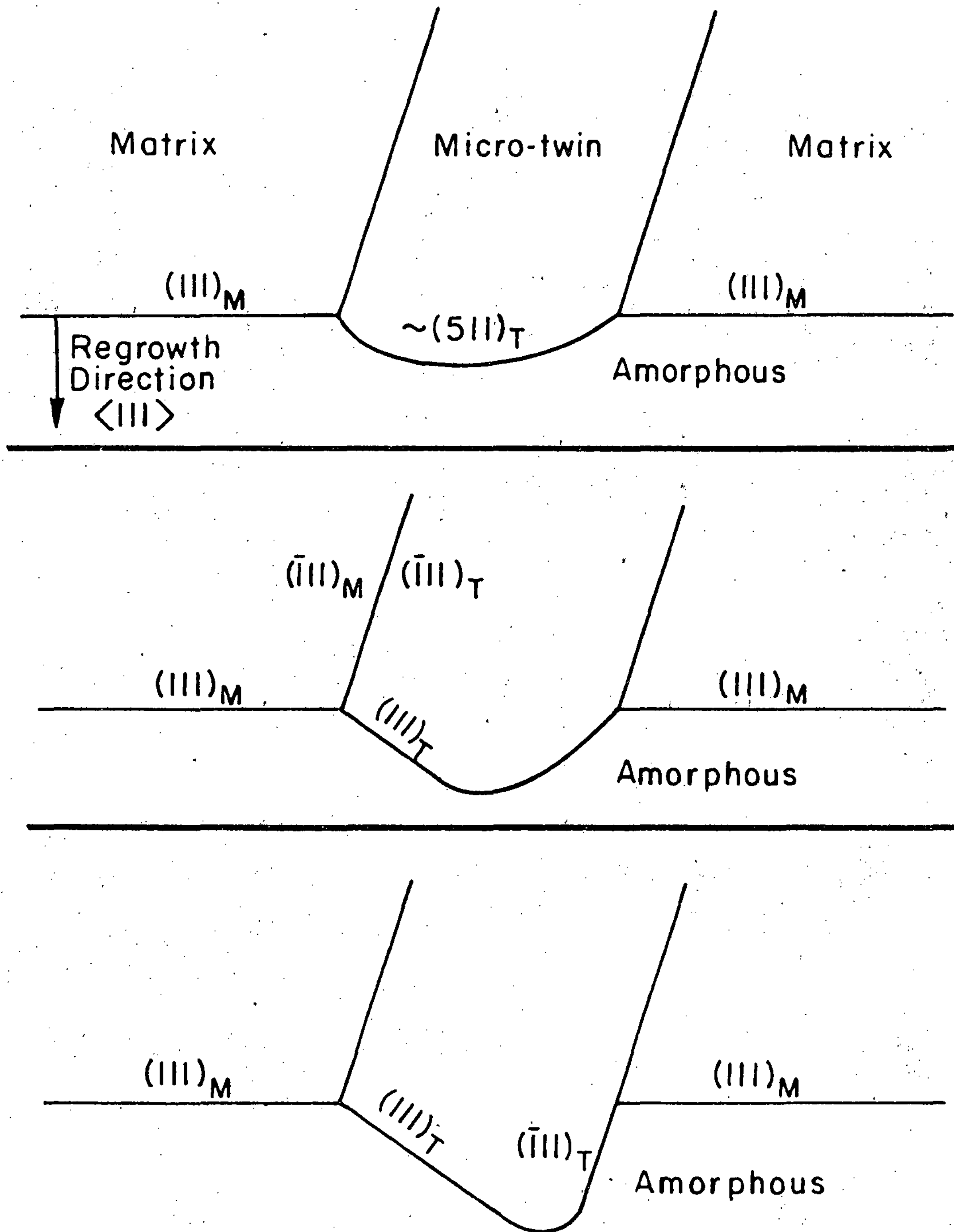

Fig. 9

XBL799-7163

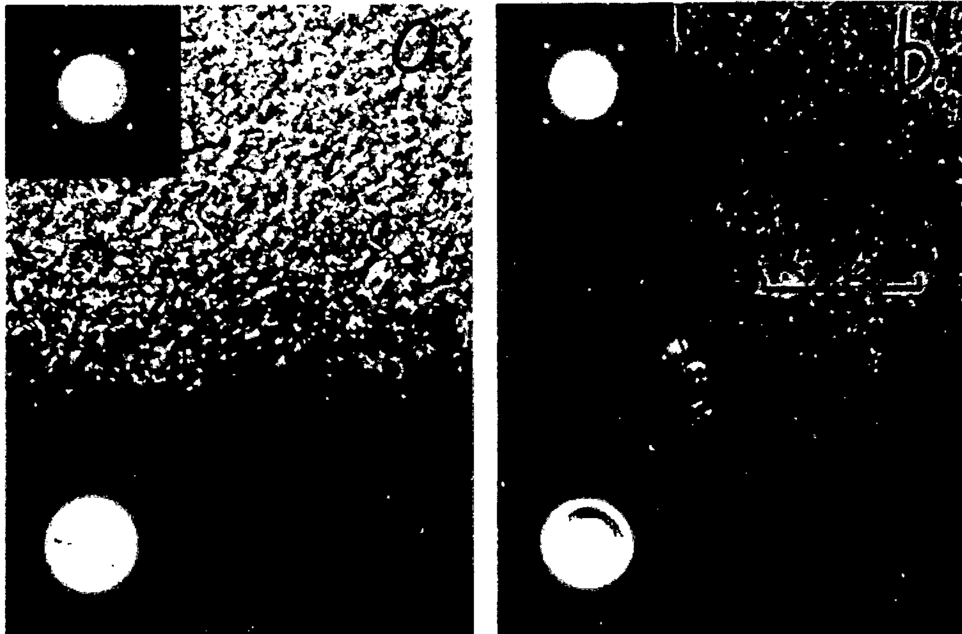

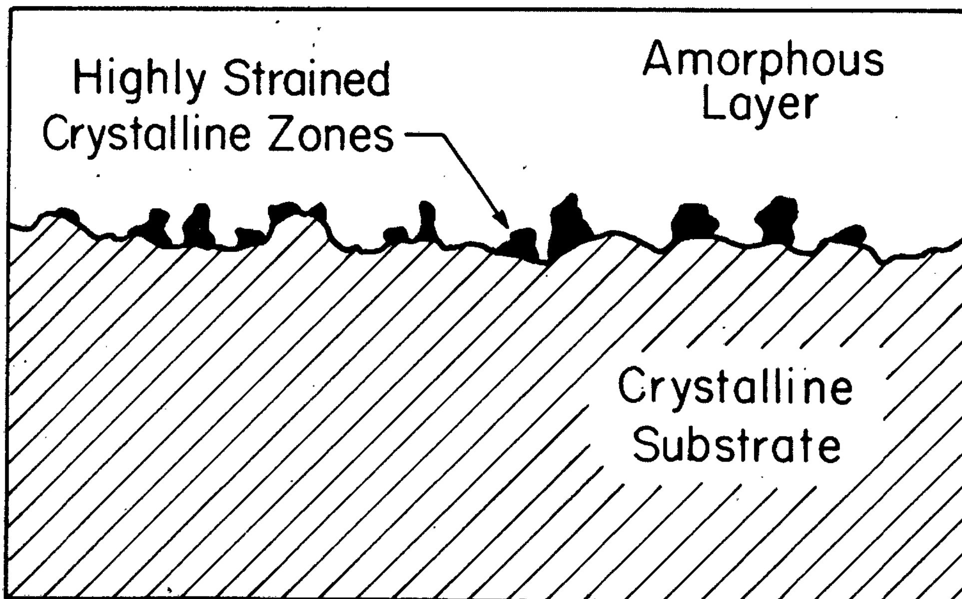

Fig. 10

XBB 802-1832

This report was done with support from the Department of Energy. Any conclusions or opinions expressed in this report represent solely those of the author(s) and not necessarily those of The Regents of the University of California, the Lawrence Berkeley Laboratory or the Department of Energy.

Reference to a company or product name does not imply approval or recommendation of the product by the University of California or the U.S. Department of Energy to the exclusion of others that may be suitable.

TECHNICAL INFORMATION DEPARTMENT
LAWRENCE BERKELEY LABORATORY
UNIVERSITY OF CALIFORNIA
BERKELEY, CALIFORNIA 94720